

# Computational Hierarchical Nanomechanics of Self-assembled Polyurea Aerogels

C. Wu\*, S. Mahadik-Khanolkar\*\*, G. Chen\* and N. Leventis\*\*

\*Department of Civil, Architectural, and Environmental Engineering, Missouri University of Science and Technology, Rolla, Missouri 65409, USA

\*\*Department of Chemistry, Missouri University of Science and Technology, Rolla, Missouri 65409, USA

## ABSTRACT

Polyurea aerogel has found its way in various engineering applications due to its multi-functionality and superior mechanical properties. In this paper, the hierarchical and self-assembling formation process of aerogel is represented by a phenomenological model. The molecular dynamics of the aerogel is computationally simulated with a united atom model in different scales. This united atom model was validated by comparing the simulated failure mechanisms and mechanical properties in uniaxial compression.

**Keywords:** Nanomechanics, Polyurea Aerogels, Molecular Dynamics, Computer Simulations

## 1 INTRODUCTION

Aerogel is an ultra-light, porous solid material formed by replacing the particles in a gel with a gas. Inorganic aerogels such as silica<sup>1</sup>, carbon, and aluminum aerogels were among the first group of inventions. These aerogels were mainly applied in various fields as thermal insulators and sometimes as dust collectors in space by NASA<sup>2</sup>. Their mechanical strength is very low.

Organic aerogels such as polyurea aerogels from isocyanates and water were more robust materials with increased mechanical strength than their inorganic counterparts<sup>3</sup>. In the late 1980s, Pekala introduced resorcinol-formaldehyde (RF) phenolic-type resins<sup>4</sup> with a record-low thermal conductivity that attracted significant attentions from the research community and broadened the subject of organic aerogels. In 2010, Leventis et al.<sup>3</sup> successfully created polyurea aerogels with cross-linking properties in primary particles. The newly formed aerogels have different morphological structures and thus mechanical properties, depending on the reaction processes with various chemical formulas.

To understand the nanostructure of the polyurea aerogels, multi-scale simulations were conducted by introducing the *ab initio* structure at atomistic level through quantum mechanical optimization, and simulating the primary and secondary particles with the so-called united atom model in molecular dynamics. Due to the structural complexity in nano-scale and difficulty to observe under a transmission electron microscopy (TEM), a phenomenological model based on the aerogel

formation mechanism was established and used to replicate the known substructure (primary particles) in computational simulations.

## 2 NANOSTRUCTURE

Depending on the amount of Desmodur N3300A in each chemical formulation, the morphology of a polyurea aerogel changes from a nano-fibrous structure to nano-particulate structure. Three types of polyurea aerogels presented in this paper all have nano-fibrous structures with 11.0 g, 16.5 g, and 24 g of Desmodur N3300A monomer dissolved in constant volume (94 ml) of dry acetone, respectively. For simplicity, these aerogels were designated as PUA-11, PUA-16, and PUA-24. It can be observed from scanning electron microscopy (SEM) images as shown in Fig. 1 that the nano-fibers were formed by the so called “secondary particles” that consists of a number of smaller “primary” particles.

The polyurea aerogel resulted from the reaction of isocyanates with water in sequence. The unstable carbamic acids in isocyanates were initially decomposed to yield amines<sup>3</sup>. The amines product further reacted with the remaining unreacted isocyanates, producing urea. Through a subsequent foaming process, these urea linkages were cross-linked and formed a primary particle. To reveal the structure of the primary particle, small angle X-ray scattering (SAXS) was conducted. Data showed that the primary particle has approximately 13 to 15 nm in radius when treated as a sphere. This observation provided a ground truth to the modeling for the chemical structure of a primary structure.

Based on the experimental data and basic monomer building block (urea, isocyanurate), the chemical structure of the polyurea aerogel is formed in “tree-growing” style as shown in Fig. 2. The primary particle starts from a core isocyanurate located at the center of the sphere, referred to as Generation 1. With the tri-functional groups attached to the core, three more isocyanurates are connected in the second layer, which is defined as Generation 2. This process continues until Generation 6 when the approximate radius of the occupied sphere after structural optimization through quantum mechanics reached the size obtained from SAXS. The process from a urea through the urea linkage to the connection of isocyanurates clearly showed that a primary particle has a hierarchy structure formation.

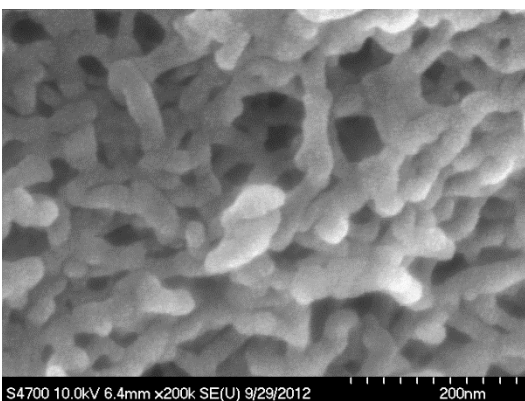


Figure 1: SEM Images of polyurea aerogel (PUA-11)

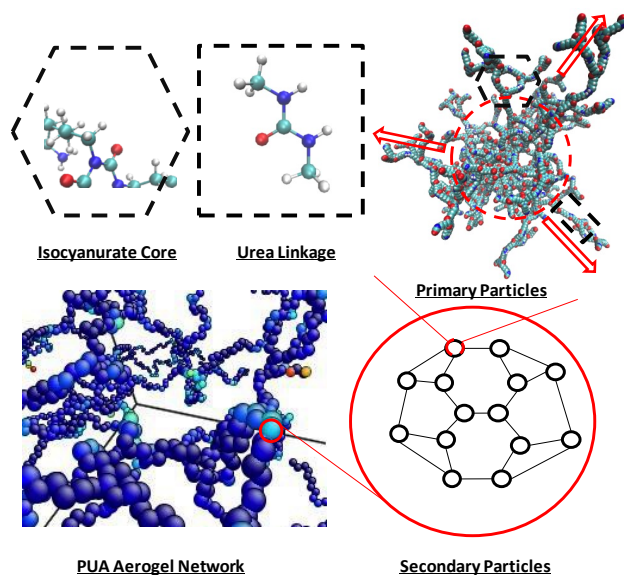


Figure 2: Nano-structure of a polyurea aerogel

The SAXS data also indicated that each secondary particle of PUA-11, PUA-16, and PUA-24 aerogels includes approximately 14-15, 18-20, and 37-39 primary particles, respectively. Fig. 2 indicated that the reactive groups in a primary particle were generally formed in three directions, representing self-similar properties in reaction from its core isocyanurate. Therefore, the network structure of a secondary particle can be formulated through sphere packing and connectivity.

### 3 PHENOMENOLOGICAL MODELING

The chemical structures of both the primary and secondary particles were described in the previous section. To complete the physical structure of a polyurea aerogel as illustrated in Fig. 3, it is hypothesized that the interaction among secondary particles is developed through induced dipole moments and collisions of unreacted functional groups from primary particles. This

hypothesis can convincingly explain the development of a fiber structure of polyurea aerogels as discussed below with a phenomenological model.

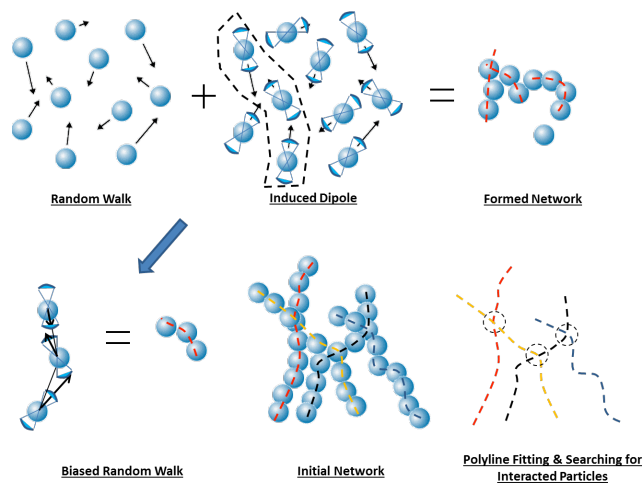


Figure 3: Formation of the network structure of a polyurea aerogel

In the proposed algorithm, each secondary particle is assigned with two conical poles randomly oriented. The angle for each conical pole is set to be  $\pi/3$  in this study. The biased-random walk enables that two particles randomly collide each other and become stabilized as they form a bond through dipole interactions. After the first cycle, fiber chains are formed with geometrical overlapping in space but no any physical connections. In this case, a trajectory line can be drawn by polynomial fitting to the centroids of the spheres along one fiber. In the computational model, the solution to a polynomial function is found by identifying and connecting the centers of many intersection sections, each formed between any two adjacent secondary particles within a search sphere centered at the intersection point (center of the intersection section) with a radius of three times of the diameter of the involved secondary particles.

## 4 MECHANICAL BEHAVIOR SIMULATION WITH MOLECULAR DYNAMICS

With rapid development of computers and computing technologies, molecular dynamics simulations gained popularity in computational mechanics as the obstacles for computational size and effort has been gradually lifted by the enhanced computing power and optimized algorithm. However, currently no molecular dynamics simulation model has been developed for polyurea aerogels. This is likely attributable to the complex nanostructure and the enormous computational effort required to effectively represent the material properties of the polyurea aerogels. For example, for a  $1 \mu\text{m}^3$  PUA-11 sample with approximately 25,000 secondary particles (90% porosity),

14 primary particles per secondary particle, and 14,000 atoms per primary particle, a total of 350 million atoms must be included in simulations when an explicit atom (EA) model is used. Therefore, to enable the understanding of structural properties based on atomic activities, simplifications must be made at different scales in multi-scale simulations. Following is a brief presentation of the procedures used in the EA model, the proposed united atom (UA) model, and the application of the UA model in multi-scale simulations.

The Dreiding force field<sup>5</sup> was applied throughout the entire simulation program. The total force field energy is expressed as:

$$E_{total} = E_{bond}(r) + E_{angle}(\theta) + E_{dihedral}(\phi) + E_{non-bonding}(r) \quad (1)$$

In this study, both bonded and non-bonded interaction potentials are considered as shown in Fig. 4. The bonded terms includes bond stretching as a function of distance  $r$  between two atoms, bond angle bending as a function of  $\theta$ , and dihedral angle torsion as a function of  $\phi$ . Each bonded term is explicitly expressed as follows:

$$E_{bond}(r) = \frac{1}{2} K_b (r - r_0)^2 \quad (2)$$

$$E_{angle}(\theta) = \frac{1}{2} K_\theta (\theta - \theta_0)^2 \quad (3)$$

$$E_{dihedral}(\phi) = \sum_{i=0}^3 C_i (\cos \phi)^i \quad (4)$$

where  $K_b$  and  $K_\theta$  are the stiffness constants for the bond stretching and angle potentials, respectively;  $r_0$  and  $\theta_0$  are the equilibrium bond length and angle, respectively; and the variable  $C_i$  represents the  $i^{\text{th}}$  dihedral multi-harmonic coefficient.

The non-bonded (van der Waals) interaction is represented by a Lennard-Jones potential,

$$E_{non-bonding}(r) = 4\epsilon \left[ \left( \frac{\sigma}{r} \right)^{12} - \left( \frac{\sigma}{r} \right)^6 \right], r \leq r_c \quad (5)$$

where  $\sigma$  is the distance between two atoms at zero energy and  $\epsilon$  is the energy well depth. The cutoff distance  $r_c$  is taken as  $10\text{\AA}$ . Based on the assumptions for Dreiding force field and the previous experience with molecular dynamics simulations of polymer materials<sup>6-12</sup>,  $K_b = 100 \text{ kcal/mol}$ ,  $K_\theta = 60 \text{ kcal/mol}$ ,  $C_0 = 1.736$ ,  $C_1 = -4.49$ ,  $C_2 = 0.776$ , and  $C_3 = 6.990 \text{ (kcal/mol)}$ . The equilibrium bond length, angle, and dihedral angle were obtained through the optimized quantum structure.

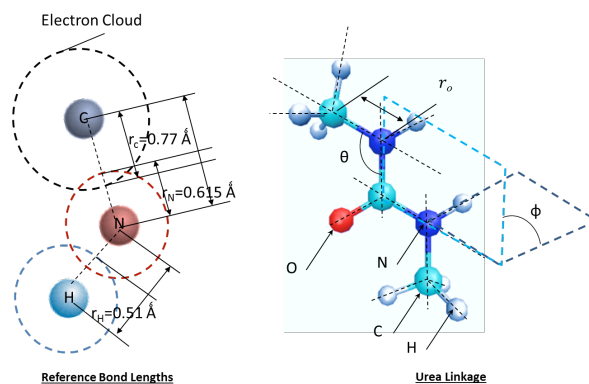


Figure 4: Reference structure and potential terms in urea linkage

The previous discussion indicated that the EA model can only be applied to understand the behavior of aerogels within a primary particle. To understand the structural behavior of aerogel materials, a united atom (UA) model is proposed in this study. The UA model becomes a natural choice in our study as it has similar force assigning system to the EA model, which will preserve the basic kinematic relationship between molecules and thus the fundamental skeleton structure and mechanical properties. However, the UA model significantly differs from the EA model in terms of computational effort since it divides a complex structure into several modules. In this case, it is crucial to differentiate the appropriate unification groups for secondary and higher level structural systems. Here, the fundamental principles in structure analysis were followed. That is, rigid components such as isocyanurate, each primary particle, and each secondary particle are modeled as solid spheres while the “soft” atom groups such as urea linkages were modeled as connectors as shown in Fig. 5. The connection between the solid spheres and the connectors were determined by various bond behaviors specified at various joints.

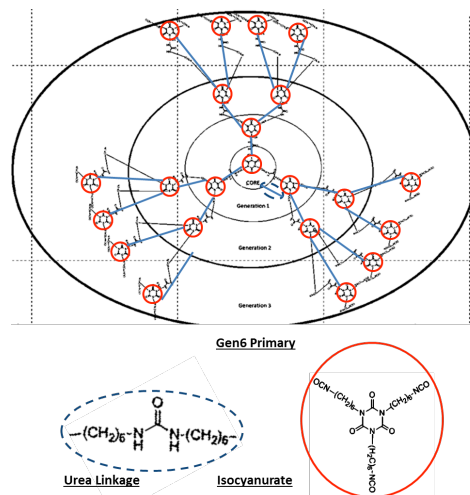


Figure 5: UA model for primary particles

The network nanostructure of polyurea aerogels was generated by the proposed phenomenological model. The connections between two secondary particles were simulated as multiple bonds between primary particles in the two secondary particles. Following the superposition principle, various bond potential terms were defined as done in the Dreiding force field research<sup>8</sup>. The non-bonded term was defined with modification according to the mass of each molecule group.

Parametric studies were conducted by varying the number of connections, the size of conics, and the average chain (stem) length. Figs. 6 presents the simulated stress-strain curves of PUA-11 aerogels (with 20,000 secondary particles) under uniaxial compression in comparison with experimental results.

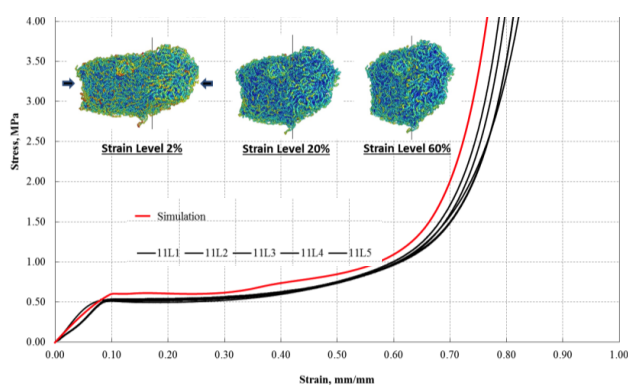


Figure 6: Simulated vs. experimental stress-strain curves of PUA-11 aerogels under uniaxial compression

Overall, the simulation results agree well with their corresponding experimental data. The slight overestimation both in stiffness and strength is likely attributable to the size effect or the simplification process made in the UA model. Similar findings were reported earlier in computational nano-mechanics of proteins where the molecular bead model similar to the UA model was adopted<sup>12</sup>. The molecular dynamical model successfully captured the collapse of nanopores and the disentanglement of networked fibers in the PUA-11 aerogel under uniaxial tension. Therefore, the proposed multi-scale modeling and simulation can accurately represent the nano-mechanics of aerogel materials.

## ACKNOWLEDGEMENT

This work is financially supported by the U.S. National Science Foundation under Award No. 1030399. The results and opinions presented in this paper are those of the authors only and do not necessarily reflect those of the sponsor.

## REFERENCES

- [1] Kistler S. S., in: Coherent Expanded Aerogels and Jellies, *Nature* 127 (3211): 741. (1931)
- [2] NASA CPL, Preventing Heat Escape Through Insulation Called Aerogel, (2004)
- [3] Leventis N., Leventis C. S., Chandrasekaran N., Mulik S., Larimore Z. J., Lu H., Churu G., and Mang J. T., in: Multifunctional Polyurea Aerogels from Isocyanates and Water. A Structure-Property Case Study, *Chem. Mater.* 22, 6692-6710, (2010)
- [4] Pekala R. W. In: Organic Aerogels from the Polycondensation of Resorcinol with Formaldehyde, *Journal of Material Science*, 24, 3221-3227, (1989)
- [5] Mayo S. L., Olafson B. D., Goddard III W. A., in: DREIDING: A Generic Force Field for Molecular Simulations, *J. Phys. Chem.* 94, 8897-8909, (1990)
- [6] Marochkin I. I., Dorofeeva O. V., in: Amine Bond Dissociation Enthalpies: Effect of Substitution on N-C Bond Strength, *Computational and Theoretical Chemistry*, 991, 182-191, (2012)
- [7] Yashiro K., Ito T., Tomita Y., in: Molecular Dynamics Simulation of Deformation Behavior in Amorphous Polymer: Nucleation of Chain Entanglements and Network Structure under Uniaxial Tension, *International Journal of Mechanical Sciences*, 45, 1863-1876, (2003)
- [8] Okumoto S., Yamabe Shinichi, in: A Computational Study of Base-Catalyzed Reactions between Isocyanates and Epoxides Affording 2-Oxazolidones and Isocyanurates, *Journal of Computational Chemistry*, Vol. 22, No. 3, 316-326 (2001)
- [9] Grujicic M., Pandurangan B., Bell W. C., Cheeseman B. A., Yen C.-F., Ranbow C. L., in: Molecular-level Simulations of Shock Generation and Propagation in Polyurea, *Materials and Science and Engineering A*, 528, 3799-3808, (2011)
- [10] Tsutsumi N., Matsumoto O., Sakai W., Kiyotsukuri T., in: Nonlinear Optical Polymers with Dipole Moment Aligned Transverse to Main Chain, *Applied Physics Letters*, 67, 2272 (1995)
- [11] Shepherd J. E., McDowell D. L., Jacob K. I. in: Modeling Morphology Evolution and Mechanical Behavior during Thermo-Mechanical Processing of Semi-Crystalline Polymers, *Journal of Mechanics and Physics of Solids*, 54, 467-489, (2006)
- [12] Buehler M. J., Keten S., Ackbarow T., in: Theoretical and Computational hierarchical Nanomechanics of Protein Materials: Deformation and Fracture, *Progress in Materials Science*, 53 1101-1241, (2008)